Detection of ^{90}Y Extravasation by Bremsstrahlung Imaging for Patients Undergoing ^{90}Y-Ibritumomab Tiuxetan Therapy

Stephanie M. Rhymer[1], J. Anthony Parker[2], and Matthew R. Palmer[2]

[1]Massachusetts College of Pharmacy and Health Sciences, Boston, Massachusetts; and [2]Division of Nuclear Medicine, Department of Radiology, Beth Israel Deaconess Medical Center, Boston, Massachusetts

Extravasation of therapeutic ^{90}Y-ibritumomab tiuxetan can cause significant injury. Detection of extravasated ^{90}Y using a γ-camera for patients undergoing ^{90}Y-ibritumomab tiuxetan therapy is a challenge because of the inherently low efficiency of bremsstrahlung imaging and the interference of prompt and scattered photons from ^{111}In that are still present in the body at the time of ^{90}Y injection. We have configured a γ-camera to image bremsstrahlung radiation from superficial ^{90}Y in the presence of ^{111}In and evaluated the effectiveness using phantoms. **Methods:** Phantoms were constructed to contain ^{90}Y and ^{111}In with activity levels and with a geometry approximating conditions in a patient being scanned for evaluation of possible extravasation in the antecubital fossa. Imaging was performed using a camera equipped with medium-energy general-purpose (MEGP) and high-energy general-purpose (HEGP) collimators. **Results:** The contrast that developed between the patch representing extravasated solution and the background was comparable for MEGP and HEGP collimators. With MEGP collimators and 5-min acquisitions, a patch containing 8.3 MBq (220 μCi) distributed over an elliptic area of 7 × 11 cm was clearly discernable. **Conclusion:** With our experimental arrangement, the lower limit of detection is approximately 8 MBq. We calculate that an extravasation of this much ^{90}Y would result in an absorbed dose to the skin and subcutaneous tissue of 2.5 Gy, which is close to the threshold for skin damage. This technique is therefore sensitive enough to be of use in the clinic when extravasation of ^{90}Y is suspected.

Key Words: radiobiology/dosimetry; radionuclide therapy; bremsstrahlung imaging; extravasation; ^{90}Y

Radioimmunotherapy is a cancer treatment modality that has grown in importance over the past decade. The combination of monoclonal antibodies and short-range radioisotopes is designed to deliver a localized radiation dose to specific targets. Used primarily in the treatment of low-grade, non-Hodgkin lymphoma, radioimmunotherapy with ^{90}Y-ibritumomab tiuxetan (Zevalin; Biogen-Idec) is approved both for first-line therapy and for relapsed or recurrent lymphoma.

The potential for complications arising from extravasation of chemotherapeutics is well understood by medical oncologists (1). Extravasation is estimated to occur in 0.6%–6% of administrations (2). In the field of nuclear medicine however, there appears to be relatively few reports of side effects caused by extravasation of radiotherapeutic agents, and the expectation and degree of vigilance for this type of reaction are generally low. The dearth of reported tissue reactions related to the administration of therapeutic agents containing ^{32}P, ^{153}Sm, ^{89}Sr, or ^{186}Re may be attributable to the short residence times due to the rapid reabsorption of those agents. In the case of ^{90}Y-ibritumomab tiuxetan, however, the large molecules could have a relatively slow clearance rate and thus pose a greater risk for radiation injury in the event of extravasation.

We previously reported on a case of radiation injury that occurred in our clinic (3). It was estimated that extravasation of between 68 and 136 MBq of ^{90}Y occurred in the antecubital fossa, resulting in an estimated absorbed dose of 20–40 Gy (3). An area of erythema was noted as soon as the following day and subsequently progressed to an 8 × 11 cm elliptic region of grade 3 dermatitis (wet desquamation).

The ^{90}Y-ibritumomab tiuxetan protocol prescribes an initial injection of ^{111}In-labled ibritumomab tiuxetan followed by imaging at 48–72 h. Provided a favorable biodistribution is observed, the patient receives the therapeutic infusion of ^{90}Y-labeled ibritumomab tiuxetan on day 7. ^{90}Y is a pure β-emitter, and imaging is challenging because of the absence of prompt γ-emission. Strategies for imaging distributions of ^{90}Y by detecting bremsstrahlung emissions have been used for various applications (4,5), but in this case, the γ-radiation from the ^{111}In, still present in the body in appreciable amounts, complicates the problem. Bremsstrahlung photons are emitted as the β-particles decelerate in tissue and form a continuous energy spectrum from zero to a

FIGURE 1. Coronal section from ^{111}In SPECT/CT study showing slice through chest and abdomen of patient 7 d after receiving ^{111}In injection. Activity is fairly uniform throughout soft tissue but is markedly concentrated in liver.

maximum of 2.3 MeV—the β-endpoint energy. The efficiency of bremsstrahlung production is low, particularly in the low-Z tissue matrix, so even at low concentrations of ^{111}In relative to ^{90}Y, the photopeaks from the ^{111}In γ-emissions at 171 and 245 keV are prominent. A technique designed to detect ^{90}Y distributions must reject those photons.

MATERIALS AND METHODS

Estimation of Relative Emissions

To establish the relative concentrations of ^{90}Y and ^{111}In and prepare a phantom to mimic the imaging environment 7 d into the ^{90}Y-ibritumomab tiuxetan protocol, we proceeded as follows. A 70-kg patient would receive a 185-MBq injection of ^{111}In for imaging and then 7 d later undergo the ^{90}Y infusion at a dose of 14.8 MBq/kg or 1.03 GBq. Assuming the worst case of no biologic decay of the ^{111}In, then at the time of ^{90}Y infusion, there remains due to physical decay 33 MBq of ^{111}In distributed in the body.

We fortuitously had available an abdominal ^{111}In SPECT/CT study obtained just before ^{90}Y infusion in a ^{90}Y-ibritumomab tiuxetan patient, that is, 7 d after injection of ^{111}In-ibritumomab tiuxetan. A coronal section through the chest and abdomen is shown in Figure 1. We observed the activity to be fairly evenly distributed in the arms and throughout the tissues of the body, with the liver having a markedly more intense activity concentration approximately 7:1 relative to the background.

Estimation of Absorbed Dose Due to Extravasation

On the basis of our experience with a single case of skin damage that resulted from extravasation of ^{90}Y, we estimated the absorbed dose to the skin as follows. The subsequent skin damage at its greatest extent was observed approximately 3 wk later as an elliptic patch measuring 7×11 cm. The maximum range of β-particles emitted by ^{90}Y is 11 mm in tissue, and the average range is 2.5 mm, with the deposited energy distributed along the particle's trajectory. From our observation of tissue damage and from a rough estimate of the depth of infusion plus a margin for β-particle range, we estimated the effective distribution of energy deposition to be an elliptic cylinder $7 \times 11 \times 1$ cm thick, for a total volume of 60 cm^3, or a total tissue mass of 0.06 kg assuming a tissue density of 1 g/cm^3. The amount of fluid extravasated into the skin of the antecubital fossa

was estimated by the staff to be between 0.5 and 1 mL of the 9-mL injection volume, which corresponds to 68–136 MBq. Based on limited data in the literature (6,7), we assumed a biologic half-life of 36 h for ^{90}Y-ibritumomab tiuxetan in tissue and thus computed a mean lifetime of 33 h. Using the energy per transition of 1.49×10^{-13} Gy·kg/Bq·s (8), we computed the corresponding absorbed dose to be 20–40 Gy.

Phantom

A phantom arrangement designed to approximate the geometry of a patient undergoing imaging to detect the presence of ^{90}Y extravasation was assembled from 3 parts: a torso phantom constructed by Data Spectrum Corp. that contains separately fillable lung and liver spaces, a cylindric tube with an inside diameter of 7.6 cm and a length of 38 cm to simulate the arm, and an elliptic 7×11 cm patch made from absorbent paper sealed between layers of plastic wrap.

The phantoms were filled with ^{111}In and ^{90}Y in amounts chosen to simulate the approximate distribution of ^{111}In and ^{90}Y expected on day 8 of the ^{90}Y-ibritumomab tiuxetan protocol, that is, immediately after infusion of ^{90}Y. The assumptions were that the liver concentrates activity in a
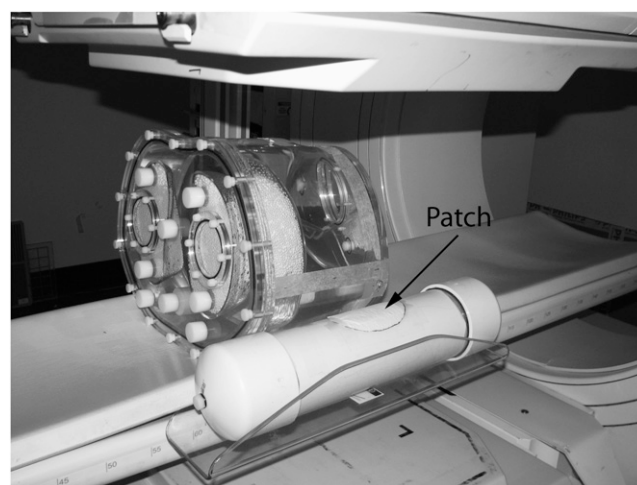
FIGURE 2. Phantom arrangement consisted of torso phantom with lung and liver inserts, and adjacent cylindric arm phantom held in arm rest. The 7×11 cm absorbent patch is visible on superior surface of cylinder.

ratio of 7:1 but activity elsewhere in the body is distributed uniformly; that the patient weighs 70 kg (volume of 70 L); and that only physical, not biologic, decay of the 185 MBq of ^{111}In injected on day 1 occurs. We thus filled the torso and arm phantoms with 0.47 and 14.8 kBq/mL activity concentrations of ^{111}In and ^{90}Y, respectively, and we filled the liver portion of the torso phantom with 7 times those concentrations.

The patches were prepared by diluting the activity into a volume of 1 mL, which we found by experimentation to be the correct quantity of liquid to just soak the absorbent paper and therefore create an elliptic region of uniform activity. Activities soaked onto the patches were 8.3, 13.7, and 26.9 MBq.

The phantoms were placed on the imaging table to simulate the geometry of a patient lying supine with arms down. The phantom arrangement in place for imaging is shown in Figure 2.

Planar Imaging

Images were acquired on the ADAC Forte dual-head γ-camera using medium-energy general-purpose (MEGP) and high-energy general-purpose (HEGP) collimators. The energy window for bremsstrahlung imaging was cen-

tered at 120 keV with a 50% window (90–150 keV). This setting accepts photons between the lead x-ray peak and the 171-keV photopeak from [111]In. This is illustrated in Figure 3. Images acquired with MEGP collimators had a matrix size of $256 \times 256 \times 16$ and an acquisition duration of 5 min. Images acquired with HEGP collimators had the same matrix size and an acquisition time of 10 min.

RESULTS

Images acquired with both sets of collimators and with the 8.3- and 26.9-MBq patches in place are shown in Figure 4. The most intense patch is clearly visible in the figure, and the least intense patch is just above the threshold of detection. We placed regions of interest on the images, and the results are graphed in Figures 5A and 5B. One region of interest was centered on the patch, and a background region of interest was placed on the arm phantom, just below the patch. Background counts were approximately 10 counts per pixel for the 5-min acquisition with MEGP collimators and 15 counts per pixel for the 10-min acquisition with HEGP collimators. As the patch activity increases, background counting rate goes up slightly for the images acquired with MEGP collimators and goes up only slightly or not at all for the HEGP collimators.

The contrast was calculated as the difference between average patch and background count densities divided by the background. This is graphed in Figure 5C, and it becomes clear that there is no contrast advantage of the HEGP collimators except perhaps for the highest-intensity patch.
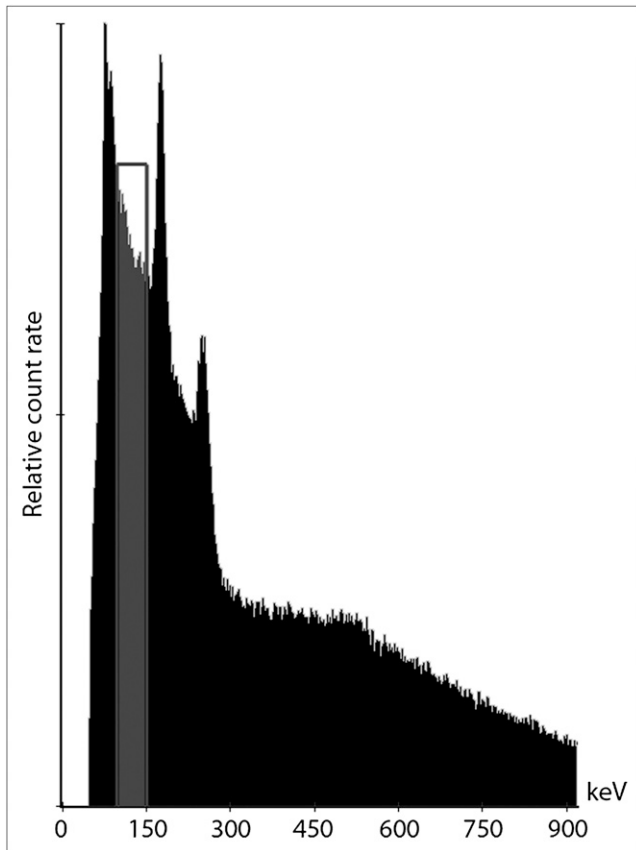
FIGURE 3. Energy window settings used for imaging bremsstrahlung photons from ^{90}Y in presence of [111]In. Window samples photons between lead x-ray peak and 171-keV photopeak from [111]In.
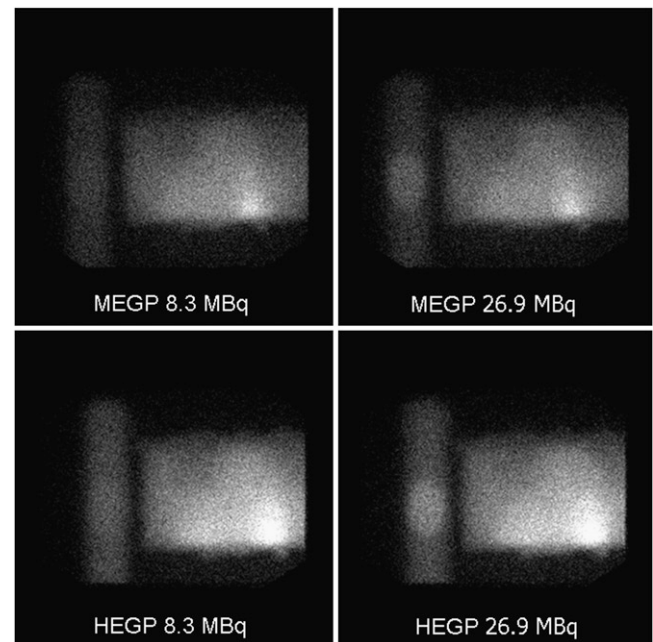
FIGURE 4. Images acquired with MEGP and HEGP collimators from phantom arrangement affixed with 8.3- and 26.9-MBq patches.
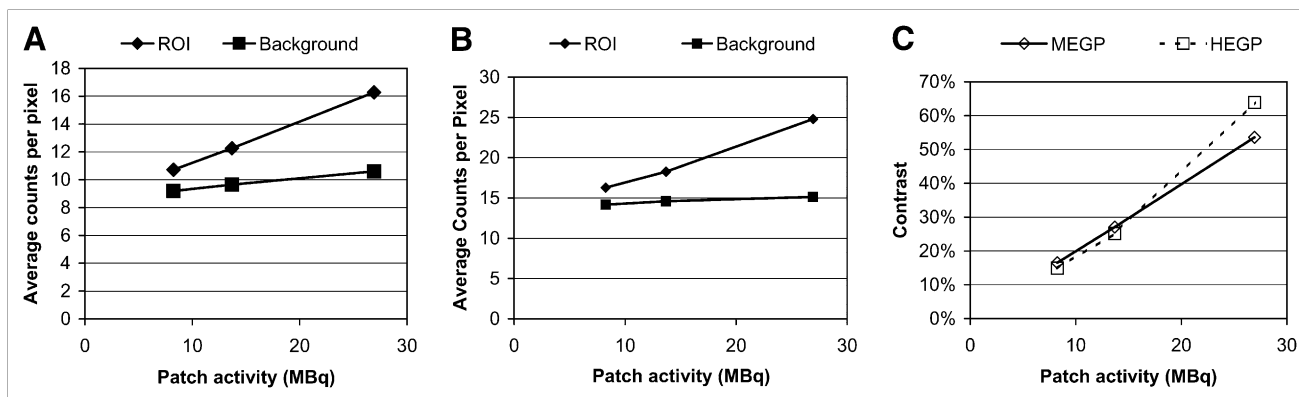
FIGURE 5. Average counts per pixel within regions of interest placed over patch and background for 3 patches containing ^{90}Y in varying concentrations for images acquired with MEGP (A) and HEGP (B) collimators. (C) Patch contrast calculated for MEGP and HEGP collimators.

DISCUSSION

Motivated by our experience of radiation-induced injury caused by extravasation of ^{90}Y-ibritumomab tiuxetan, we sought to design and evaluate an imaging scheme sensitive enough to detect the bremsstrahlung radiation emitted by ^{90}Y but insensitive to ^{111}In γ-emission, which forms an appreciable background 7 d after injection. The approach we have taken uses a standard γ-camera with MEGP collimators and with the energy window set to detect photons in the range of 90–150 keV. This window overlaps a region of relatively high bremsstrahlung radiation while avoiding lead x-rays on one end and the 171-keV photopeak from ^{111}In decay on the other end.

Our phantom was designed to mimic, to some degree, the conditions expected 7 d into the ^{90}Y-ibritumomab tiuxetan protocol, after ^{90}Y infusion, when a suspected extravasation would be investigated. The concentration and distribution of ^{111}In and ^{90}Y were estimated from limited clinical observations, as was the distribution pattern of ^{90}Y extravasation. With this phantom arrangement, we demonstrated that we could detect extravasation in the area of the antecubital fossa down to an activity of about 8 MBq. Of course in practice, there would be a great deal of variability associated with these conditions, making a precise determination of the limits of detection difficult. In our phantom acquisitions, by arranging the torso next to the arm instead of mimicking an extended arm, and by distributing the ^{90}Y extravasation over a relatively large area (extravasation might be expected to be initially less dispersed), we have mimicked a worst-case scenario. It may well be possible to detect activity lower than 8 MBq.

Using the same model for the geometry and clearance of extravasation as we used previously, we can calculate that an extravasation of 8 MBq of ^{90}Y would result in an absorbed dose of 2.4 Gy to the skin and subcutaneous tissue. Thus, we surmise from these estimates that we can

image ^{90}Y, in the presence of residual ^{111}In, with a lower limit of detection that is close to the threshold for radiation damage. For the lowest activities tested, a MEGP collimator produced at least as great a contrast relative to background in a shorter acquisition time.

CONCLUSION

We have evaluated the ability to imaging bremsstrahlung from ^{90}Y in the presence of ^{111}In in a phantom study designed to mimic extravasated ^{90}Y-ibritumomab tiuxetan immediately after injection. With MEGP collimators and a 5-min acquisition time on a conventional γ-camera, extravasation can be detected at the approximate concentration that would be expected to cause skin damage. This technique is therefore sensitive enough to be of use in the clinic when extravasation of ^{90}Y-ibritumomab tiuxetan is suspected.

REFERENCES

1. Ener RA, Meglathery S, Styler M. Extravasation of systemic hemato-oncological therapies. *Ann Oncol.* 2004;15:858–862.
2. Jordan K, Grothe W, Schmoll HJ. Extravasation of chemotherapeutic agents: prevention and therapy. *Dtsch Med Wochenschr.* 2005;130:33–37.
3. Williams G, Palmer MR, Parker JA, Joyce R. Extravazation of therapeutic yttrium-90-ibritumomab tiuxetan (Zevalin): a case report. *Cancer Biother Radiopharm.* 2006;21:101–105.
4. Shen S, DeNardo GL, Yuan A, DeNardo DA, DeNardo SJ. Planar gamma camera imaging and quantitation of yttrium-90 bremsstrahlung. *J Nucl Med.* 1994; 35:1381–1389.
5. Qian W, Clarke LP. A restoration algorithm for P-32 and Y-90 bremsstrahlung emission nuclear imaging: a wavelet-neural network approach. *Med Phys.* 1996; 23:1309–1323.
6. Wiseman GA, Kornmehl E, Leigh B, et al. Radiation dosimetry results and safety correlations from ^{90}Y-ibritumomab tiuxetan radioimmunotherapy for relapsed or refractory non-Hodgkin's lymphoma: combined data from 4 clinical trials. *J Nucl Med.* 2003;44:465–474.
7. Shen S, Forero A, Meredith RF, et al. Impact of rituximab treatment on ^{90}Y-ibritumomab dosimetry for patients with non-Hodgkin lymphoma. *J Nucl Med.* 2010;51:150–157.
8. Eckerman KF, Endo A. *MIRD: Radionuclide Data and Decay Schemes.* 2nd ed. Reston, VA: Society of Nuclear Medicine; 2008.